Structural Monitoring and Maintenance, *Vol. 7, No. 2 (2020) 85-107*
DOI: https://doi.org/10.12989/smm.2020.7.2.085

Numerical investigation on scale-dependent vibrations of porous foam plates under dynamic loads

Raad M. Fenjan[1], Ridha A. Ahmed[1], Nadhim M. Faleh[*2] and Fatima Masood Hani[1]

[1]Al-Mustansiriah University, Engineering Collage P.O. Box 46049, Bab-Muadum, Baghdad 10001, Iraq
[2]Ministry of construction and housing, Iraq

(Received July 29, 2019, Revised March 16, 2020, Accepted March 17, 2020)

Abstract. Dynamic responses of porous piezoelectric and metal foam nano-size plates have been examined via a four variables plate formulation. Diverse pore dispersions named uniform, symmetric and asymmetric have been selected. The piezoelectric nano-size plate is subjected to an external electrical voltage. Nonlocal strain gradient theory (NSGT) which includes two scale factors has been utilized to provide size-dependent model of foam nanoplate. The presented plate formulation verifies the shear deformations impacts and it gives fewer number of field components compared to first-order plate model. Hamilton's principle has been utilized for deriving the governing equations. Achieved results by differential quadrature (DQ) method have been verified with those reported in previous studies. The influences of nonlocal factor, strain gradients, electrical voltage, dynamical load frequency and pore type on forced responses of metal and piezoelectric foam nano-size plates have been researched.

Keywords: response; piezoelectric; electric voltage; wave; piezoelectric plate

1. Introduction

Piezoelectric foam and metal foam are in the category of smart and porous materials with low weight due to possessing different variations of porosities in them (Ahmed *et al*. 2019, Al-Maliki *et al*. 2019). Applying electric field to piezoelectric material structures yields elastic deformations and changed vibrational properties. The variation of porosities in this material causes a significant difference between metal foams and other perfect metals. In a non-perfect metal, the material characteristics are notably influenced by pore variations. Also, this variation in pores can affect the vibration frequencies of engineering structures made of metal foams. This issue can be understood from the works done by Chen *et al.* (2015, 2016). Different from metal foams, there are also functionally graded (FG) or ceramic-metal materials in which pore variation effect is very important (Medani *et al*. 2019, Meksi *et al*. 2019, Mahmoudi *et al.* 2019). In this material, pores may be produced in a phase between ceramic and material (Ait Atmane *et al.* 2017, Attia *et al.* 2018, Addou *et al.* 2019). Engineering structures made of this materials are studied to understand their vibration behaviors as reported in the works of Wattanasakulpong *et al*. (2014), Yahia *et al*. (2015), Atmane *et al*. (2015). Most recently, Ebrahimi *et al.* (2019) studied free vibrations of metal foam cylindrical

∗Corresponding author, Professor, E-mail: dr.nadhim@uomustansiriyah.edu.iq

http://www.techno-press.org/?journal=smm&subpage=7 ISSN: 2288-6605 (Print), 2288-6613 (Online)

shells with different porosity distributions.

Recent studies focus on engineering structures at nano-scales due to their involvement in nano-mechanical systems or devices (Ebrahimi and Barati 2016, Li *et al.* 2013, Liu *et al.* 2016). However, the main issue in these studies is to select an appropriate elasticity theory accounting for small scale impacts. The impact of size-dependency might be considered with the help of a scale parameter involved in non-local theory of elasticity Eringen (1983). The word "non-local" means that the stresses are not local anymore. This is because we are talking about a stress field of nano-scale structure. Many authors are aware of these facts and they are using this theory to analysis mechanical characteristics of small size engineering structures (Eltaher *et al.* 2016, Natarajan *et al.* 2012, Elmerabet *et al.* 2017, Zenkour and Abouelregal 2015, Sobhy and Radwan 2017, El-Hassar *et al.* 2016, Fenjan *et al.* 2019, Merazi *et al*. 2015, Sadoun *et al.* 2018, Sayyad and Ghugal 2018). Different values for nonlocal parameter are considered in research studies (Li *et al.* 2019). Related to the mechanics of porous functionally graded nano-size structures, there are some studies about their vibrations or buckling in the literature such as the paper of Mechab *et al*. (2016). These papers showed that pores inside FG material can cause extraordinary dynamic and static properties.

Strain gradients at nano-scale are observed by many researchers (Lim *et al.* 2015). Thus, nonlocal-strain gradient theory was introduced as a general theory which contains an additional strain gradient parameter together with nonlocal parameter (Li and Hu 2016, Xiao *et al.* 2017, Zhou and Li 2017). The scale parameters used in nonlocal strain gradient theory can be obtained by fitting obtained theoretical results with available experimental data and even molecular dynamic (MD) simulations.

In the present paper, dynamical responses of a porous FGM nanoplates subjected to out-of-plane harmonic and in-plane thermo-electric loads have been explored employing a four variables plate formulation based upon exact location of neutral surface. Suggested formulation verifies the shear deformations impacts and includes fewer number of field variables compared to first-order and improved 5-unknown plate formulations. Higher order theories are suitable for thicker structures needless of shear correction factor. Some functions have been applied for expressing the pore-dependent material characteristics. The nanoplate's equations are arranged in the forms of ordinary equations via DQ method to derive amplitude-frequency curves. Detailed effects of dynamical loading factors, nonlocal factor, foundation factors, and pores on amplitude-frequency curves of FGM nano-sized plates are explored.

2. Nanoplate modeling based on NSGT

In the well-known nonlocal strain gradient theory (Lim *et al.* 2015), strain gradient impacts are taken into accounting together with nonlocal stress influences defined in below relation

$$\sigma_{ij} = \sigma_{ij}^{(0)} - \nabla \sigma_{ij}^{(1)} \tag{1}$$

in such a way that stress $\sigma_{ij}^{(0)}$ is corresponding to strain components ε_{kl} and a higher order stress is related to strain gradient components $\nabla\varepsilon_{kl}$ which are (Lim *et al*. 2015)

$$\sigma_{ij}^{(0)} = \int_V C_{ijkl}\alpha_0(x, x', e_0a)\varepsilon'_{kl}(x')dx' \tag{2a}$$

$$\sigma_{ij}^{(1)} = l^2 \int_V C_{ijkl} \alpha_1(x, x', e_1 a) \nabla \varepsilon'_{kl}(x') dx' \tag{2b}$$

in which C_{ijkl} express the elastic properties; Also, $e_0 a$ and $e_1 a$ are corresponding to nonlocality impacts (Semmah *et al*. 2019, Yazid *et al*. 2018) and l is related to strains gradients. Whenever two nonlocality functions $\alpha_0(x, x', e_0 a)$ and $\alpha_1(x, x', e_1 a)$ verify Eringen's announced conditions, NSGT constitutive relation may be written as follows

$$[1-(e_1 a)^2 \nabla^2][1-(e_0 a)^2 \nabla^2]\sigma_{ij} = C_{ijkl}[1-(e_1 a)^2 \nabla^2]\varepsilon_{kl} - C_{ijkl}\, l^2 [1-(e_0 a)^2 \nabla^2]\nabla^2 \varepsilon_{kl} \tag{3}$$

so that ∇^2 defines the operator for Laplacian; by selecting $e_1 = e_0 = e$, above relationship decreases to

$$[1-(ea)^2 \nabla^2]\sigma_{ij} = C_{ijkl}\, [1 - l^2 \nabla^2]\varepsilon_{kl} \tag{4}$$

3. Porous nanoplate model with different porosity distributions

A porous material, for instance a steel foam, might be placed in the category of lightweight materials and can be applied in several structures such as sandwich panels. Often, pore variation along the thickness of panels/plates results in a notable alteration in every kind of material property. When the pore distribution inside the material is selected to be non-uniform, the metal foam might be defined as a functionally graded material since its properties obey some specified functions. Herein, the following types of pore dispersion will be employed

- Uniform kind

$$E = E_2(1 - e_0 \chi) \tag{5a}$$

$$\alpha = \alpha_2(1 - e_0 \chi) \tag{5b}$$

$$\rho = \rho_2 \sqrt{(1 - e_0 \chi)} \tag{5c}$$

- Non-uniform kind 1

$$E(z) = E_2 (1 - e_0 \cos\left(\frac{\pi z}{h}\right)) \tag{6a}$$

$$\alpha(z) = \alpha_2 (1 - e_0 \cos\left(\frac{\pi z}{h}\right)) \tag{6b}$$

$$\rho(z) = \rho_2 (1 - e_m \cos\left(\frac{\pi z}{h}\right)) \tag{6c}$$

- Non-uniform kind 2

$$E(z)=E_2(1-e_0\cos\left(\frac{\pi z}{2h}+\frac{\pi}{4}\right)) \tag{7a}$$

$$\alpha(z)=\alpha_2(1-e_0\cos\left(\frac{\pi z}{2h}+\frac{\pi}{4}\right)) \tag{7b}$$

$$\rho(z)=\rho_2(1-e_m\cos\left(\frac{\pi z}{2h}+\frac{\pi}{4}\right)) \tag{7c}$$

The most important factors in above relations are the greatest values of material properties E_2, α_2 and ρ_2. For a piezoelectric foam all material properties (*P*) including elastic constants (c_{ij}), piezo-electric constants (e_{ij}) and dielectric coefficients (k_{ij}) can be described via the function $P=P_2(1-e_0\chi)$ for uniform porosities and $P=P_2(1-e_0\cos\left(\frac{\pi z}{h}\right))$ for non-uniform porosities. Also, there are two important factors related to pores and mass which are e_0 and e_m as

$$e_0=1-\frac{E_2}{E_1}=1-\frac{G_2}{G_1} \tag{8a}$$

$$e_m=1-\frac{\rho_2}{\rho_1} \tag{8b}$$

Based on the open cell assumption of porous material, we use the following relations

$$\frac{E_2}{E_1}=\left(\frac{\rho_2}{\rho_1}\right)^2 \tag{9a}$$

$$e_m=1-\sqrt{1-e_0} \tag{9b}$$

Based on uniformly distributed pores, the following parameter is used in Eq. (5) as

$$\chi=\frac{1}{e_0}-\frac{1}{e_0}\left(\frac{2}{\pi}\sqrt{1-e_0}-\frac{2}{\pi}+1\right)^2 \tag{10}$$

By defining exact location of neutral surface, the displacement components based on axial *u*, lateral *v*, bending w_b and shear w_s displacements may be introduced as

$$u_x(x,y,z,t)=u(x,y,t)-(z-r^*)\frac{\partial w_b}{\partial x}-[\Upsilon(z)-r^{**}]\frac{\partial w_s}{\partial x} \tag{11a}$$

$$u_y\left(x,y,z,t\right)=v\left(x,y,t\right)-(z-r^{*})\frac{\partial w_b}{\partial y}-[\Upsilon(z)-r^{**}]\frac{\partial w_s}{\partial y} \tag{11b}$$

$$u_z(x,y,z,t)=w(x,y,t)=w_b+w_s \tag{11c}$$

so that

$$\begin{aligned} r^{*} &= \int_{-h/2}^{h/2} E(z)\,z dz \Big/ \int_{-h/2}^{h/2} E(z)\,dz \\ r^{**} &= \int_{-h/2}^{h/2} E(z)\,\Upsilon(z) dz \Big/ \int_{-h/2}^{h/2} E(z)\,dz \end{aligned} \tag{12}$$

Here, third order shear function is employed as

$$\Upsilon(z)=-\frac{z}{4}+\frac{5z^3}{3h^2} \tag{13}$$

Accordingly, we can calculate the components of the strain field based upon the four variables plate assumptions

$$\begin{aligned} \varepsilon_x &= \frac{\partial u}{\partial x}-(z-r^{*})\frac{\partial^2 w_b}{\partial x^2}-[\Upsilon(z)-r^{**}]\frac{\partial^2 w_s}{\partial x^2} \\ \varepsilon_y &= \frac{\partial v}{\partial y}-(z-r^{*})\frac{\partial^2 w_b}{\partial y^2}-[\Upsilon(z)-r^{**}]\frac{\partial^2 w_s}{\partial y^2} \\ \gamma_{xy} &= \frac{\partial u}{\partial y}+\frac{\partial v}{\partial x}-2(z-r^{*})\frac{\partial^2 w_b}{\partial x\partial y}-2[\Upsilon(z)-r^{**}]\frac{\partial^2 w_s}{\partial x\partial y} \\ \gamma_{yz} &= g(z)\frac{\partial w_s}{\partial y}, \quad \gamma_{xz}=g(z)\frac{\partial w_s}{\partial x} \end{aligned} \tag{14}$$

Considering the fact that foam nanoplate is under electrical field with electrical potential (Φ), one can define the potential in following form as functions of electrical voltage (V_E)

$$\Phi(x,y,z,t)=-\cos(\xi z)\phi(x,y,t)+\frac{2z}{h}V_E \tag{15}$$

with $\xi=\pi/h$. Calculating the three-dimensional gradient of electrical potential gives the electrical field components (E_x, E_y, E_z) as follows

$$E_x=-\Phi_{,x}=\cos(\xi z)\frac{\partial\phi}{\partial x}, \tag{16a}$$

$$E_y=-\Phi_{,y}=\cos(\xi z)\frac{\partial\phi}{\partial y}, \tag{16b}$$

$$E_z=-\Phi_{,z}=-\xi\sin(\xi z)\phi-\frac{2V_E}{h} \tag{16c}$$

Next, one might express the Hamilton's rule as follows based on strain energy (U) and kinetic energy (T)

$$\int_0^t \delta(U-T-V)\,dt = 0 \tag{17}$$

and V is the work of non-conservative loads. Based on above relation we have

$$\begin{aligned}\delta U = \int_V (&\sigma_{xx}\delta\varepsilon_{xx} + \sigma_{xx}^{(1)}\delta\nabla\varepsilon_{xx} + \sigma_{yy}\delta\varepsilon_{yy} + \sigma_{yy}^{(1)}\delta\nabla\varepsilon_{yy} + \sigma_{xy}\delta\gamma_{xy} + \sigma_{xy}^{(1)}\delta\nabla\gamma_{xy}\\ &+\sigma_{yz}\delta\gamma_{yz} + \sigma_{yz}^{(1)}\delta\nabla\gamma_{yz} + \sigma_{xz}\delta\gamma_{xz} + \sigma_{xz}^{(1)}\delta\nabla\gamma_{xz} - D_x\delta E_x - D_y\delta E_y - D_z\delta E_z)\,dV\end{aligned} \tag{18a}$$

Placing Eq. (14) in Eq.(18(a)) leads to

$$\begin{aligned}\delta U = &\int_0^a\int_0^b [N_{xx}[\frac{\partial\delta u}{\partial x} + \frac{\partial w}{\partial x}\frac{\partial\delta w}{\partial x}] - M_{xx}^b\frac{\partial^2\delta w_b}{\partial x^2} - M_{xx}^s\frac{\partial^2\delta w_s}{\partial x^2} + N_{yy}[\frac{\partial\delta v}{\partial y} + \frac{\partial w}{\partial y}\frac{\partial\delta w}{\partial y}]\\ &- M_{yy}^b\frac{\partial^2\delta w_b}{\partial y^2} - M_{yy}^s\frac{\partial^2\delta w_s}{\partial y^2} + N_{xy}(\frac{\partial\delta u}{\partial y} + \frac{\partial\delta v}{\partial x} + \frac{\partial w}{\partial x}\frac{\partial\delta w}{\partial y} + \frac{\partial w}{\partial y}\frac{\partial\delta w}{\partial x}) - 2M_{xy}^b\frac{\partial^2\delta w_b}{\partial x\partial y}\\ &-2M_{xy}^s\frac{\partial^2\delta w_s}{\partial x\partial y} + Q_{yz}\frac{\partial\delta w_s}{\partial y} + Q_{xz}\frac{\partial\delta w_s}{\partial x}]dydx\\ &+\int_0^a\int_0^b\int_{-h/2}^{h/2}\left(-D_x\cos(\xi z)\,\delta\left(\frac{\partial\phi}{\partial x}\right) - D_y\cos(\xi z)\,\delta\left(\frac{\partial\phi}{\partial y}\right) + D_z\xi\sin(\xi z)\,\delta\phi\right)dzdydx\end{aligned} \tag{18b}$$

in which

$$\begin{aligned}
N_{xx} &= \int_{-h/2}^{h/2}(\sigma_{xx}^0 - \nabla\sigma_{xx}^{(1)})dz = N_{xx}^{(0)} - \nabla N_{xx}^{(1)}\\
N_{xy} &= \int_{-h/2}^{h/2}(\sigma_{xy}^0 - \nabla\sigma_{xy}^{(1)})dz = N_{xy}^{(0)} - \nabla N_{xy}^{(1)}\\
N_{yy} &= \int_{-h/2}^{h/2}(\sigma_{yy}^0 - \nabla\sigma_{yy}^{(1)})dz = N_{yy}^{(0)} - \nabla N_{yy}^{(1)}\\
M_{xx}^b &= \int_{-h/2}^{h/2} z(\sigma_{xx}^0 - \nabla\sigma_{xx}^{(1)})dz = M_{xx}^{b(0)} - \nabla M_{xx}^{b(1)}\\
M_{xx}^s &= \int_{-h/2}^{h/2} f(\sigma_{xx}^0 - \nabla\sigma_{xx}^{(1)})dz = M_{xx}^{s(0)} - \nabla M_{xx}^{s(1)}\\
M_{yy}^b &= \int_{-h/2}^{h/2} z(\sigma_{yy}^0 - \nabla\sigma_{yy}^{(1)})dz = M_{yy}^{b(0)} - \nabla M_{yy}^{b(1)}\\
M_{yy}^s &= \int_{-h/2}^{h/2} f(\sigma_{yy}^0 - \nabla\sigma_{yy}^{(1)})dz = M_{yy}^{s(0)} - \nabla M_{yy}^{s(1)}\\
M_{xy}^b &= \int_{-h/2}^{h/2} z(\sigma_{xy}^0 - \nabla\sigma_{xy}^{(1)})dz = M_{xy}^{b(0)} - \nabla M_{xy}^{b(1)}\\
M_{xy}^s &= \int_{-h/2}^{h/2} f(\sigma_{xy}^0 - \nabla\sigma_{xy}^{(1)})dz = M_{xy}^{s(0)} - \nabla M_{xy}^{s(1)}\\
Q_{xz} &= \int_{-h/2}^{h/2} g(\sigma_{xz}^0 - \nabla\sigma_{xz}^{(1)})dz = Q_{xz}^{(0)} - \nabla Q_{xz}^{(1)}\\
Q_{yz} &= \int_{-h/2}^{h/2} g(\sigma_{yz}^0 - \nabla\sigma_{yz}^{(1)})dz = Q_{yz}^{(0)} - \nabla Q_{yz}^{(1)}
\end{aligned} \tag{19a}$$

where

$$
\begin{aligned}
&N_{ij}^{(0)}=\int_{-h/2}^{h/2}(\sigma_{ij}^{(0)})dz, \quad N_{ij}^{(1)}=\int_{-h/2}^{h/2}(\sigma_{ij}^{(1)})dz\\
&M_{ij}^{b(0)}=\int_{-h/2}^{h/2}z(\sigma_{ij}^{b(0)})dz, \quad M_{ij}^{b(1)}=\int_{-h/2}^{h/2}z(\sigma_{ij}^{b(1)})dz\\
&M_{ij}^{s(0)}=\int_{-h/2}^{h/2}f(\sigma_{ij}^{s(0)})dz, \quad M_{ij}^{s(1)}=\int_{-h/2}^{h/2}f(\sigma_{ij}^{s(1)})dz\\
&Q_{xz}^{(0)}=\int_{-h/2}^{h/2}g(\sigma_{xz}^{i(0)})dz, \quad Q_{xz}^{(1)}=\int_{-h/2}^{h/2}g(\sigma_{xz}^{i(1)})dz\\
&Q_{yz}^{(0)}=\int_{-h/2}^{h/2}g(\sigma_{yz}^{i(0)})dz, \quad Q_{yz}^{(1)}=\int_{-h/2}^{h/2}g(\sigma_{yz}^{i(1)})dz
\end{aligned} \tag{19b}
$$

for which (*ij=xx, xy, yy*). The variation for the work of non-conservative force is expressed by

$$
\begin{aligned}
\delta V=\int_0^a\int_0^b (&N_x^0\frac{\partial(w_b+w_s)}{\partial x}\frac{\partial\delta(w_b+w_s)}{\partial x}+N_y^0\frac{\partial(w_b+w_s)}{\partial y}\frac{\partial\delta(w_b+w_s)}{\partial y}\\
&+2\delta N_{xy}^0\frac{\partial(w_b+w_s)}{\partial x}\frac{\partial(w_b+w_s)}{\partial y}-(k_w-q_{dynamic})(w_b+w_s)\delta(w_b+w_s)\\
&+(k_p-(N^E+N^T))(\frac{\partial(w_b+w_s)}{\partial x}\frac{\partial\delta(w_b+w_s)}{\partial x}+\frac{\partial(w_b+w_s)}{\partial y}\frac{\partial\delta(w_b+w_s)}{\partial y}))dydx
\end{aligned} \tag{20}
$$

where N_x^0, N_y^0, N_{xy}^0 denote membrane forces; k_w, k_p are elastic substrate constants. Moreover, $q_{dynamic}$ is the applied force from periodic mechanical loading. Also, the kinetic energy variation is obtained as

$$
\begin{aligned}
\delta K=\int_0^a\int_0^b[&I_0(\frac{\partial u}{\partial t}\frac{\partial\delta u}{\partial t}+\frac{\partial v}{\partial t}\frac{\partial\delta v}{\partial t}+\frac{\partial(w_b+w_s)}{\partial t}\frac{\partial\delta(w_b+w_s)}{\partial t})-I_1(\frac{\partial u}{\partial t}\frac{\partial\delta w_b}{\partial x\partial t}+\frac{\partial w_b}{\partial x\partial t}\frac{\partial\delta u}{\partial t}+\frac{\partial v}{\partial t}\frac{\partial\delta w_b}{\partial y\partial t}\\
&+\frac{\partial w_b}{\partial y\partial t}\frac{\partial\delta v}{\partial t})-I_2(\frac{\partial u}{\partial t}\frac{\partial\delta w_s}{\partial x\partial t}+\frac{\partial w_s}{\partial x\partial t}\frac{\partial\delta u}{\partial t}+\frac{\partial v}{\partial t}\frac{\partial\delta w_s}{\partial y\partial t}+\frac{\partial w_s}{\partial y\partial t}\frac{\partial\delta v}{\partial t})+I_3(\frac{\partial w_b}{\partial x\partial t}\frac{\partial\delta w_b}{\partial x\partial t}+\frac{\partial w_b}{\partial y\partial t}\frac{\partial\delta w_b}{\partial y\partial t})\\
&+I_4(\frac{\partial w_s}{\partial x\partial t}\frac{\partial\delta w_s}{\partial x\partial t}+\frac{\partial w_s}{\partial y\partial t}\frac{\partial\delta w_s}{\partial y\partial t})+I_5(\frac{\partial w_b}{\partial x\partial t}\frac{\partial\delta w_s}{\partial x\partial t}+\frac{\partial w_s}{\partial x\partial t}\frac{\partial\delta w_b}{\partial x\partial t}+\frac{\partial w_b}{\partial y\partial t}\frac{\partial\delta w_s}{\partial y\partial t}+\frac{\partial w_s}{\partial y\partial t}\frac{\partial\delta w_b}{\partial y\partial t})]dydx
\end{aligned} \tag{21a}
$$

in which

$$
(I_0,I_1,I_2,I_3,I_4,I_5)=\int_{-h/2}^{h/2}(1,z-z^*,(z-z^*)^2,f-z^{**},(z-z^*)(f-z^{**}),(f-z^{**})^2)\rho(z)dz \tag{21b}
$$

Substituting Eqs. (18)-(21) into Eq. (17) then collecting the coefficients for field variables results in four equations of motion for piezoelectric plates

$$\frac{\partial N_x}{\partial x}+\frac{\partial N_{xy}}{\partial y}=I_0\frac{\partial^2 u}{\partial t^2}-I_1\frac{\partial^3 w_b}{\partial x\partial t^2}-I_3\frac{\partial^3 w_s}{\partial x\partial t^2} \tag{22a}$$

$$\frac{\partial N_{xy}}{\partial x}+\frac{\partial N_y}{\partial y}=I_0\frac{\partial^2 v}{\partial t^2}-I_1\frac{\partial^3 w_b}{\partial y\partial t^2}-I_3\frac{\partial^3 w_s}{\partial y\partial t^2} \tag{22b}$$

$$\begin{aligned}&\frac{\partial^2 M_x^b}{\partial x^2}+2\frac{\partial^2 M_{xy}^b}{\partial x\partial y}+\frac{\partial^2 M_y^b}{\partial y^2}-k_w(w_b+w_s)+k_p\nabla^2(w_b+w_s)-(N^E+N^T)\nabla^2(w_b+w_s)-q_{dynamic}\\&=+I_0\frac{\partial^2(w_b+w_s)}{\partial t^2}+I_1(\frac{\partial^3 u}{\partial x\partial t^2}+\frac{\partial^3 v}{\partial y\partial t^2})-I_2\nabla^2(\frac{\partial^2 w_b}{\partial t^2})-I_4\nabla^2(\frac{\partial^2 w_s}{\partial t^2})\end{aligned} \tag{22c}$$

$$\begin{aligned}&\frac{\partial^2 M_x^s}{\partial x^2}+2\frac{\partial^2 M_{xy}^s}{\partial x\partial y}+\frac{\partial^2 M_y^s}{\partial y^2}+\frac{\partial Q_{xz}}{\partial x}+\frac{\partial Q_{yz}}{\partial y}-k_w(w_b+w_s)-(N^E+N^T)\nabla^2(w_b+w_s)-q_{dynamic}\\&+k_p\nabla^2(w_b+w_s)=I_0\frac{\partial^2(w_b+w_s)}{\partial t^2}+I_3(\frac{\partial^3 u}{\partial x\partial t^2}+\frac{\partial^3 v}{\partial y\partial t^2})-I_4\nabla^2(\frac{\partial^2 w_b}{\partial t^2})-I_5\nabla^2(\frac{\partial^2 w_s}{\partial t^2})\end{aligned} \tag{22d}$$

$$\int_{-h/2}^{h/2}\left(\cos(\xi z)\frac{\partial D_x}{\partial x}+\cos(\xi z)\frac{\partial D_y}{\partial y}+\xi\sin(\xi z)D_z\right)dz=0 \tag{22e}$$

in which electric force may be defined as $N^E=\int_{-h/2}^{h/2}\tilde{e}_{31}\frac{2V_E}{h}dz$. Thermal load can be calculates as $N^T=\int_{-h/2}^{h/2}\tilde{c}_{11}\,\alpha\Delta T\,dz$. Also, note that for a metal foam plate the piezoelectric effect must be neglected and therefore Eq. (22(e)) must be deleted.

Next, all edge conditions for $x=0$, a and $y=0$, b may be expressed by (Draiche *et al.* 2016)

$$\text{Specify } w_b \text{ or } \left(\frac{\partial M_{xx}^b}{\partial x}+\frac{\partial M_{xy}^b}{\partial y}\right)n_x+\left(\frac{\partial M_{yy}^b}{\partial y}+\frac{\partial M_{xy}^b}{\partial x}\right)n_y=0$$

$$\left(\frac{\partial M_{xx}^s}{\partial x}+\frac{\partial M_{xy}^s}{\partial y}+Q_{xz}\right)n_x+\left(\frac{\partial M_{yy}^s}{\partial y}+\frac{\partial M_{xy}^s}{\partial x}+Q_{yz}\right)n_y=0 \tag{23a}$$

$$\text{Specify } \frac{\partial w_b}{\partial n} \text{ or } M_{xx}^b n_x^2+n_x n_y M_{xy}^b+M_{yy}^b n_y^2=0$$

Note that $\frac{\partial()}{\partial n}=n_x\frac{\partial()}{\partial x}+n_y\frac{\partial()}{\partial y}$; n_x and n_y respectively define axial and lateral normal vectors at edges, and non-classic edge condition may be written as

$$\text{Specify } \frac{\partial^2 w_b}{\partial x^2} \text{ or } M_{xx}^{b(1)}=0$$

$$\text{Specify } \frac{\partial^2 w_b}{\partial y^2} \text{ or } M_{yy}^{b(1)}=0 \tag{23b}$$

$$\text{Specify } \frac{\partial^2 w_s}{\partial x^2} \text{ or } M_{xx}^{s(1)} = 0$$
$$\text{Specify } \frac{\partial^2 w_s}{\partial y^2} \text{ or } M_{yy}^{s(1)} = 0$$

Furthermore, we can define the relations between the stresses and the strain field based upon the four variables plate assumptions

$$(1-\mu\nabla^2)\begin{Bmatrix}\sigma_x\\ \sigma_y\\ \sigma_{xy}\\ \sigma_{yz}\\ \sigma_{xz}\end{Bmatrix} = \frac{E(z)}{1-\nu^2}(1-\lambda\nabla^2)\begin{pmatrix}1 & \nu & 0 & 0 & 0\\ \nu & 1 & 0 & 0 & 0\\ 0 & 0 & (1-\nu)/2 & 0 & 0\\ 0 & 0 & 0 & (1-\nu)/2 & 0\\ 0 & 0 & 0 & 0 & (1-\nu)/2\end{pmatrix}\begin{Bmatrix}\varepsilon_x\\ \varepsilon_y\\ \gamma_{xy}\\ \gamma_{yz}\\ \gamma_{xz}\end{Bmatrix} \tag{24}$$

For a piezoelectric foam nanoplate, the constitutive relations become

$$(1-\mu\nabla^2)\sigma_{xx} = (1-\lambda\nabla^2)[\tilde{c}_{11}\varepsilon_{xx} + \tilde{c}_{12}\varepsilon_{yy}] - \tilde{e}_{31}E_z \tag{25a}$$

$$(1-\mu\nabla^2)\sigma_{yy} = (1-\lambda\nabla^2)[\tilde{c}_{12}\varepsilon_{xx} + \tilde{c}_{11}\varepsilon_{yy}] - \tilde{e}_{31}E_z \tag{25b}$$

$$(1-\mu\nabla^2)\sigma_{xy} = (1-\lambda\nabla^2)\tilde{c}_{66}\gamma_{xy} \tag{25c}$$

$$(1-\mu\nabla^2)\sigma_{xz} = \tilde{c}_{55}(1-\lambda\nabla^2)\gamma_{xz} - \tilde{e}_{15}E_x \tag{25d}$$

$$(1-\mu\nabla^2)\sigma_{yz} = \tilde{c}_{55}(1-\lambda\nabla^2)\gamma_{yz} - \tilde{e}_{15}E_x \tag{25e}$$

$$(1-\mu\nabla^2)D_x = \tilde{e}_{15}(1-\lambda\nabla^2)\gamma_{xz} + \tilde{k}_{11}E_x \tag{25f}$$

$$(1-\mu\nabla^2)D_y = \tilde{e}_{15}(1-\lambda\nabla^2)\gamma_{yz} + \tilde{k}_{11}E_y \tag{25g}$$

$$(1-\mu\nabla^2)D_z = \tilde{e}_{31}(1-\lambda\nabla^2)\varepsilon_{xx} + \tilde{e}_{31}(1-\lambda\nabla^2)\varepsilon_{yy} + \tilde{k}_{33}E_z \tag{25h}$$

So that

$$\begin{gathered}\tilde{c}_{11} = c_{11} - \frac{c_{13}^2}{c_{33}},\ \tilde{c}_{12} = c_{12} - \frac{c_{13}^2}{c_{33}},\ \tilde{c}_{66} = c_{66}\\ \tilde{e}_{31} = e_{31} - \frac{c_{13}e_{33}}{c_{33}},\ \tilde{k}_{11} = k_{11},\ \tilde{k}_{33} = k_{33} + \frac{e_{33}^2}{c_{33}}\end{gathered} \tag{26}$$

After integrating Eq. (24) in thickness direction, we get to the following relationships

$$(1-\mu\nabla^2)\begin{Bmatrix} N_x \\ N_y \\ N_{xy} \end{Bmatrix} = A(1-\lambda\nabla^2)\begin{pmatrix} 1 & v & 0 \\ v & 1 & 0 \\ 0 & 0 & (1-v)/2 \end{pmatrix}\begin{Bmatrix} \frac{\partial u}{\partial x} \\ \frac{\partial v}{\partial y} \\ \frac{\partial u}{\partial y}+\frac{\partial v}{\partial x} \end{Bmatrix} \tag{27}$$

$$(1-\mu\nabla^2)\begin{Bmatrix} M_x^b \\ M_y^b \\ M_{xy}^b \end{Bmatrix} = D(1-\lambda\nabla^2)\begin{pmatrix} 1 & v & 0 \\ v & 1 & 0 \\ 0 & 0 & (1-v)/2 \end{pmatrix}\begin{Bmatrix} -\frac{\partial^2 w_b}{\partial x^2} \\ -\frac{\partial^2 w_b}{\partial y^2} \\ -2\frac{\partial^2 w_b}{\partial x\partial y} \end{Bmatrix} + E(1-\lambda\nabla^2)\begin{pmatrix} 1 & v & 0 \\ v & 1 & 0 \\ 0 & 0 & (1-v)/2 \end{pmatrix}\begin{Bmatrix} -\frac{\partial^2 w_s}{\partial x^2} \\ -\frac{\partial^2 w_s}{\partial y^2} \\ -2\frac{\partial^2 w_s}{\partial x\partial y} \end{Bmatrix} \tag{28}$$

$$(1-\mu\nabla^2)\begin{Bmatrix} M_x^s \\ M_y^s \\ M_{xy}^s \end{Bmatrix} = E(1-\lambda\nabla^2)\begin{pmatrix} 1 & v & 0 \\ v & 1 & 0 \\ 0 & 0 & (1-v)/2 \end{pmatrix}\begin{Bmatrix} -\frac{\partial^2 w_b}{\partial x^2} \\ -\frac{\partial^2 w_b}{\partial y^2} \\ -2\frac{\partial^2 w_b}{\partial x\partial y} \end{Bmatrix} + F(1-\lambda\nabla^2)\begin{pmatrix} 1 & v & 0 \\ v & 1 & 0 \\ 0 & 0 & (1-v)/2 \end{pmatrix}\begin{Bmatrix} -\frac{\partial^2 w_s}{\partial x^2} \\ -\frac{\partial^2 w_s}{\partial y^2} \\ -2\frac{\partial^2 w_s}{\partial x\partial y} \end{Bmatrix} \tag{29}$$

$$(1-\mu\nabla^2)\begin{Bmatrix} Q_x \\ Q_y \end{Bmatrix} = A_{44}(1-\lambda\nabla^2)\begin{pmatrix} 1 & 0 \\ 0 & 1 \end{pmatrix}\begin{Bmatrix} \frac{\partial w_s}{\partial x} \\ \frac{\partial w_s}{\partial y} \end{Bmatrix} \tag{30}$$

in which

$$\begin{gathered} A=\int_{-h/2}^{h/2}\frac{E(z)}{1-v^2}dz,\quad D=\int_{-h/2}^{h/2}\frac{E(z)(z-r^*)^2}{1-v^2}dz,\quad E=\int_{-h/2}^{h/2}\frac{E(z)(z-r^*)(\Upsilon-r^{**})}{1-v^2}dz \\ F=\int_{-h/2}^{h/2}\frac{E(z)(\Upsilon-r^{**})^2}{1-v^2}dz,\quad A_{44}=\int_{-h/2}^{h/2}\frac{E(z)}{2(1+v)}g^2dz \end{gathered} \tag{31}$$

Two equations of motion for metal foam plate based on neutral surface location will be achieved by placing Eqs. (27)-(30) in Eqs. (22) by

$$\begin{gathered} -D(1-\lambda\nabla^2)(\frac{\partial^4 w_b}{\partial x^4}+2\frac{\partial^4 w_b}{\partial x^2\partial y^2}+\frac{\partial^4 w_b}{\partial y^4})-E(1-\lambda\nabla^2)(\frac{\partial^4 w_s}{\partial x^4}+2\frac{\partial^4 w_s}{\partial x^2\partial y^2}+\frac{\partial^4 w_s}{\partial y^4}) \\ +(1-\mu\nabla^2)(-I_0\frac{\partial^2(w_b+w_s)}{\partial t^2}+I_2\nabla^2(\frac{\partial^2 w_b}{\partial t^2})+I_4\nabla^2(\frac{\partial^2 w_s}{\partial t^2}) \\ -k_w(w_b+w_s)+k_p\nabla^2(w_b+w_s))=q_{dynamic}-\mu\frac{\partial^2 q_{dynamic}}{\partial x^2} \end{gathered} \tag{32}$$

$$-E(1-\lambda\nabla^2)(\frac{\partial^4 w_b}{\partial x^4}+2\frac{\partial^4 w_b}{\partial x^2\partial y^2}+\frac{\partial^4 w_b}{\partial y^4})-F(1-\lambda\nabla^2)(\frac{\partial^4 w_s}{\partial x^4}+2\frac{\partial^4 w_s}{\partial x^2\partial y^2}+\frac{\partial^4 w_s}{\partial y^4})$$
$$+A_{44}(1-\lambda\nabla^2)(\frac{\partial^2 w_s}{\partial x^2}+\frac{\partial^2 w_s}{\partial y^2})+(1-\mu\nabla^2)(-I_0\frac{\partial^2(w_b+w_s)}{\partial t^2} \tag{33}$$
$$+I_4\nabla^2(\frac{\partial^2 w_b}{\partial t^2})+I_5\nabla^2(\frac{\partial^2 w_s}{\partial t^2})-k_w(w_b+w_s)+k_p\nabla^2(w_b+w_s))=q_{dynamic}-\mu\frac{\partial^2 q_{dynamic}}{\partial x^2}$$

For the piezoelectric foam nanoplate, the governing equations discarding in-plane displacements become

$$+(1-\lambda\nabla^2)[-D_{11}\frac{\partial^4 w_b}{\partial x^4}-2(D_{12}+2D_{66})\frac{\partial^4 w_b}{\partial x^4\partial y^2}-D_{22}\frac{\partial^4 w_b}{\partial y^4}-D_{11}^s\frac{\partial^4 w_s}{\partial x^4}$$
$$-2(D_{12}^s+2D_{66}^s)\frac{\partial^4 w_s}{\partial x^4\partial y^2}-D_{22}^s\frac{\partial^4 w_s}{\partial y^4}]+E_{31}^e\nabla^2\phi+(1-\mu\nabla^2)[+I_0\frac{\partial^2(w_b+w_s)}{\partial t^2}+I_1(\frac{\partial^3 u}{\partial x\partial t^2}+\frac{\partial^3 v}{\partial y\partial t^2}) \tag{34}$$
$$-I_2\nabla^2(\frac{\partial^2 w_b}{\partial t^2})-J_2\nabla^2(\frac{\partial^2 w_s}{\partial t^2})-(N^E+N^T)\nabla^2(w_b+w_s)]=q_{dynamic}-\mu\frac{\partial^2 q_{dynamic}}{\partial x^2}$$

$$+(1-\lambda\nabla^2)[-D_{11}^s\frac{\partial^4 w_b}{\partial x^4}+A_{55}^s\frac{\partial^2 w_s}{\partial x^2}+A_{44}^s\frac{\partial^2 w_s}{\partial y^2}-2(D_{12}^s+2D_{66}^s)\frac{\partial^4 w_b}{\partial x^4\partial y^2}-D_{22}^s\frac{\partial^4 w_b}{\partial y^4}$$
$$-H_{11}^s\frac{\partial^4 w_s}{\partial x^4}-2(H_{12}^s+2H_{66}^s)\frac{\partial^4 w_s}{\partial x^4\partial y^2}-H_{22}^s\frac{\partial^4 w_s}{\partial y^4}]+F_{31}^e\nabla^2\phi+(1-\mu\nabla^2)[+I_0\frac{\partial^2(w_b+w_s)}{\partial t^2} \tag{35}$$
$$+J_1(\frac{\partial^3 u}{\partial x\partial t^2}+\frac{\partial^3 v}{\partial y\partial t^2})-J_2\nabla^2(\frac{\partial^2 w_b}{\partial t^2})$$
$$-K_2\nabla^2(\frac{\partial^2 w_s}{\partial t^2})-(N^E+N^T)\nabla^2(w_b+w_s)]-A_{15}^e\nabla^2\phi=q_{dynamic}-\mu\frac{\partial^2 q_{dynamic}}{\partial x^2}$$

$$-E_{31}^e\nabla^2 w_b-F_{31}^e\nabla^2 w_s+E_{15}^e\nabla^2 w_s+F_{11}^e\nabla^2\phi-F_{33}^e\phi=0 \tag{36}$$

So that

$$\begin{Bmatrix} A_{11}, B_{11}, B_{11}^s, D_{11}, D_{11}^s, H_{11}^s \\ A_{12}, B_{12}, B_{12}^s, D_{12}, D_{12}^s, H_{12}^s \\ A_{66}, B_{66}, B_{66}^s, D_{66}, D_{66}^s, H_{66}^s \end{Bmatrix}=\int_A \begin{Bmatrix} \tilde{c}_{11} \\ \tilde{c}_{12} \\ \tilde{c}_{66} \end{Bmatrix}(1, z, f, z^2, zf, f^2)\,dA \tag{37}$$

$$\left\{A_{31}^e, E_{31}^e, F_{31}^e\right\}=\int_{-h/2}^{h/2}\tilde{e}_{31}\xi\sin(\xi z)\left\{1, z, f\right\}dz \tag{38}$$

$$\left\{A_{15}^e, E_{15}^e\right\}=\int_{-h/2}^{h/2}\tilde{e}_{15}\cos(\xi z)\left\{1, g\right\}dz \tag{39}$$

$$\left\{F_{11}^e, F_{33}^e\right\}=\int_{-h/2}^{h/2}\left\{\tilde{k}_{11}\cos^2(\xi z), \tilde{k}_{33}\xi^2\sin^2(\xi z)\right\}dz \tag{40}$$

$$A_{44}^s=A_{55}^s=\int_A \tilde{c}_{55}g^2 dA \tag{41}$$

4. Solution by differential quadrature method (DQM)

In the present chapter, differential quadrature method (DQM) has been utilized for solving the governing equations for NSGT porous FG nanoplate. According to DQM, at an assumed grid point (x_i, y_j) the derivatives for function F are supposed as weighted linear summation of all functional values within the computation domains as

$$\frac{d^nF}{dx^n}\Big|_{x=x_i} = \sum_{j=1}^{N} c_{ij}^{(n)} F(x_j) \tag{42}$$

where

$$C_{ij}^{(1)} = \frac{\pi(x_i)}{(x_i - x_j)\ \pi(x_j)} \qquad i, j = 1,2, \ldots, N, \qquad i \neq j \tag{43}$$

in which $\pi(x_i)$ is defined by

$$\pi(x_i) = \prod_{j=1}^{N} (x_i - x_j), \qquad i \neq j \tag{44}$$

And when $i = j$

$$C_{ij}^{(1)} = c_{ii}^{(1)} = -\sum_{k=1}^{N} C_{ik}^{(1)}, \qquad i = 1,2, \ldots, N, \qquad i \neq k,\ i = j \tag{45}$$

Then, weighting coefficients for high orders derivatives may be expressed by

$$\begin{aligned}
C_{ij}^{(2)} &= \sum_{k=1}^{N} C_{ik}^{(1)} C_{kj}^{(1)} \\
C_{ij}^{(3)} &= \sum_{k=1}^{N} C_{ik}^{(1)} C_{kj}^{(2)} = \sum_{k=1}^{N} C_{ik}^{(2)} C_{kj}^{(1)} \\
C_{ij}^{(4)} &= \sum_{k=1}^{N} C_{ik}^{(1)} C_{kj}^{(3)} = \sum_{k=1}^{N} C_{ik}^{(3)} C_{kj}^{(1)} \qquad i, j = 1, 2, \ldots, N. \\
C_{ij}^{(5)} &= \sum_{k=1}^{N} C_{ik}^{(1)} C_{kj}^{(4)} = \sum_{k=1}^{N} C_{ik}^{(4)} C_{kj}^{(1)} \\
C_{ij}^{(6)} &= \sum_{k=1}^{N} C_{ik}^{(1)} C_{kj}^{(5)} = \sum_{k=1}^{N} C_{ik}^{(5)} C_{kj}^{(1)}
\end{aligned} \tag{46}$$

According to presented approach, the dispersions of grid points based upon Gauss-Chebyshev-Lobatto assumption are expressed as

$$\begin{aligned}
x_i &= \frac{a}{2}\left[1 - \cos\left(\frac{i-1}{N-1}\pi\right)\right] \qquad i = 1, 2, \ldots, N, \\
y_j &= \frac{b}{2}\left[1 - \cos\left(\frac{j-1}{M-1}\pi\right)\right] \qquad j = 1, 2, \ldots, M,
\end{aligned} \tag{47}$$

Next, the time derivative for displacement components may be determined by

$$w_b(x,y,t) = W_b(x,y)e^{i\omega t} \tag{48}$$

$$w_s(x,y,t) = W_s(x,y)e^{i\omega t} \tag{49}$$

$$\phi(x,y,t) = \Phi_{mn}(x,y)e^{i\omega t} \tag{50}$$

where W_b and W_n denote vibration amplitudes and ω defines the vibrational frequency. Then, it is possible to express obtained boundary conditions as

$$\begin{gathered}\phi = w_b = w_s = 0,\\ \frac{\partial^2 w_b}{\partial x^2} = \frac{\partial^2 w_s}{\partial x^2} = \frac{\partial^2 w_b}{\partial y^2} = \frac{\partial^2 w_s}{\partial y^2} = 0\\ \frac{\partial^4 w_b}{\partial x^4} = \frac{\partial^4 w_s}{\partial x^4} = \frac{\partial^4 w_b}{\partial y^4} = \frac{\partial^4 w_s}{\partial y^4} = 0\end{gathered} \tag{51}$$

Now, one can express the modified weighting coefficients for all edges simply-supported as

$$\begin{aligned}&\bar{C}_{1,j}^{(2)} = \bar{C}_{N,j}^{(2)} = 0, \qquad i = 1,2,\dots,M,\\ &\bar{C}_{i,1}^{(2)} = \bar{C}_{1,M}^{(2)} = 0, \qquad i = 1,2,\dots,N.\end{aligned} \tag{52}$$

and

$$\bar{C}_{ij}^{(3)} = \sum_{k=1}^{N} C_{ik}^{(1)}\bar{C}_{kj}^{(2)} \qquad \bar{C}_{ij}^{(4)} = \sum_{k=1}^{N} C_{ik}^{(1)}\bar{C}_{kj}^{(3)} \tag{53}$$

By substituting Eqs. (48)-(50) into Eqs. (34) and (36), and using the DQM, one obtains

$$\left\{[K] + \omega_{ex}^2[M]\right\}\begin{Bmatrix} W_{bmn}\\ W_{smn}\\ \Phi_{mn}\end{Bmatrix} = \begin{Bmatrix} Q_{dynamic}\\ Q_{dynamic}\\ 0\end{Bmatrix} \tag{54}$$

in which ω_{ex} is the excitation frequency. Six grid points are adequate for convergence of the method. The presented results are based on the below dimensionless factors

$$\begin{gathered}K_w = \frac{k_w a^4}{D_2}, K_0 = \frac{k_0 a^4}{D_2}, K_p = \frac{k_p a^2}{D_2}, D_1 = \frac{E_2 h^3}{12(1-v^2)},\ \mu = \frac{ea}{a},\ \lambda = \frac{l}{a}\\ \Omega = \omega_{ex} a\sqrt{\frac{\rho_2}{E_2}}\ , \Omega = \omega_{ex}\frac{a^2}{h}\sqrt{\frac{\rho_2}{c_{11}}}\ , \bar{W}_{uniform} = W\frac{10E_2 h^3}{a^4 q_0}\end{gathered} \tag{55}$$

Table 1 Electro-mechanical coefficients of material properties of piezoelectric material.

Properties	PZT-4
$c_{11} = c_{22}$ (GPa)	138.499
c_{12}	77.371
c_{13}	73.643
c_{33}	114.745
c_{55}	25.6
c_{66}	30.6
e_{31} ($\mathrm{Cm^{-2}}$)	-5.2
e_{33}	15.08
e_{15}	12.72
k_{11} ($\mathrm{C^2 m^{-2} N^{-1}}$)	1.306e-9
k_{33}	1.115e-9
$\alpha(1/K)$	2e-6
ρ ($\mathrm{kgm^{-3}}$)	7600

5. Discussions on results

Thorough the present section, results are provided for forced vibration investigation of scale-dependent piezoelectric and metal foam plates formulated by a four-unknown plate theory and NSGT. The nano-size foam plate under a periodic dynamical loading has been depicted in Fig. 2. Table 1 presents material coefficients for the piezoelectric PZT material. Table 2 provides validation study for vibrational frequency of a functionally graded small scale plate with the results obtained by Natarajan *et al*. (2012). Accordingly, the present formulation and DQ solution is capable of giving accurate results of nanoplates. In this research, obtained results based on metal foam material are presented using the below properties

- $E_2 = 200\ GPa,\ \rho_2 = 7850\ kg/m^3,\ v = 0.33,$

In Fig. 3, the variation of normalized deflections of a metal foam nano-dimension plate versus excitation frequency of mechanical loading is represented for several nonlocality (μ) and stain gradients (λ) coefficients when *a/h*=10. By selecting μ= λ=0, the deflections and vibrational frequencies based upon classic plate assumption will be derived. Actually, selecting λ=0 gives the deflections in the context of nonlocal elasticity theory and discarding strain gradients impacts. Exerting higher values of excitation frequency leads to larger deflections and finally resonance of the plate. It can be understand from Fig. 3 that normalized deflection of system will reduce with strain gradient coefficient and will rise with nonlocality coefficient. This observation is valid for excitation frequencies before resonance. So, forced vibration behavior of the nanoplate system is dependent on both scale effects. An important finding is that the resonance frequencies of metal foam plate are outstandingly affected by the values of nonlocal and strain gradient coefficients.

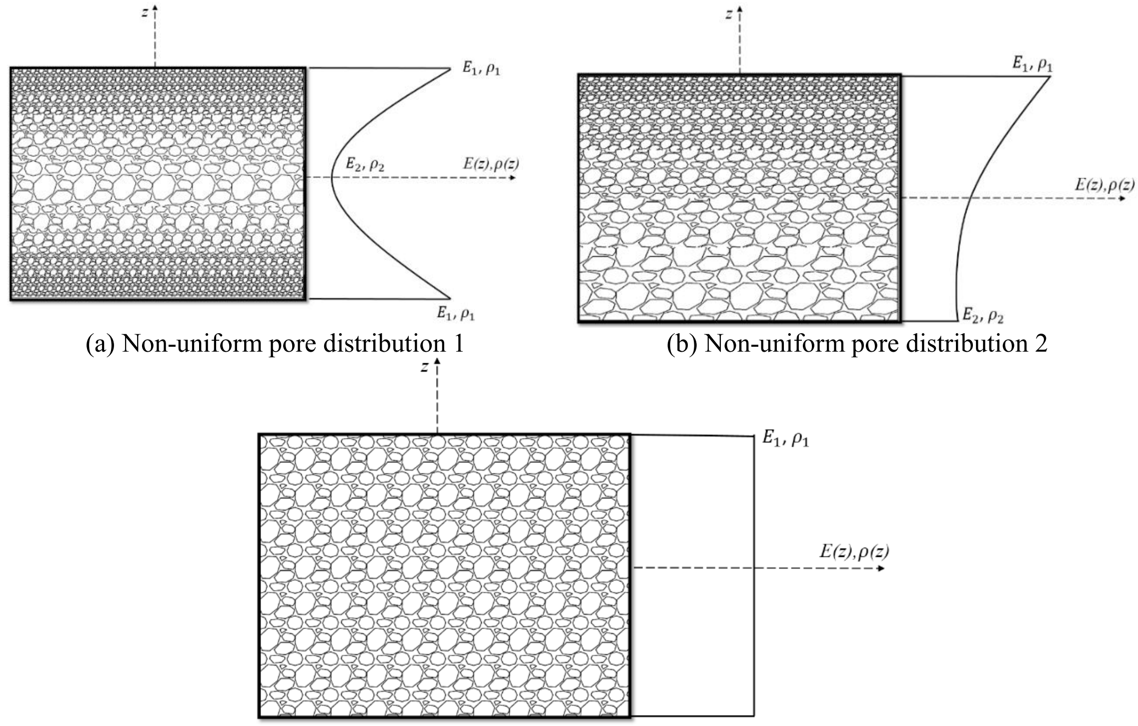

(a) Non-uniform pore distribution 1 (b) Non-uniform pore distribution 2

(c) Uniform pore distribution

Fig. 1 Pore types along the thickness direction

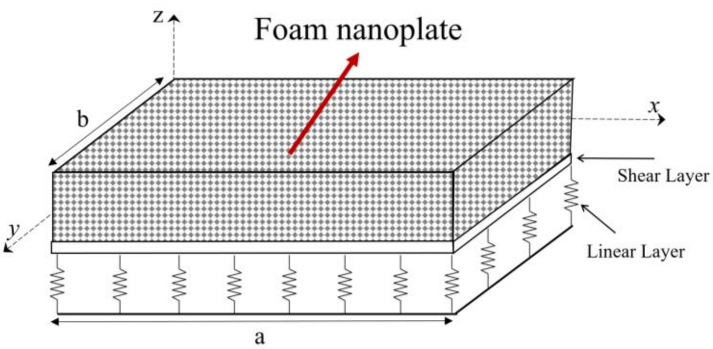

Fig. 2 Configuration of foam nanoplate under dynamical loading

Effect of applied electric voltage on the variation of normalized deflections of a piezoelectric foam nano-dimension plate versus excitation frequency of mechanical loading is illustrated in Fig. 4. Uniform porosities with e_0=0.2 inside piezoelectric foam have been assumed. One can see that applying negative electrical voltages to a nano-scale plate causes greater resonance vibration frequencies than applying a positive electrical voltage. Such observation is because of raised

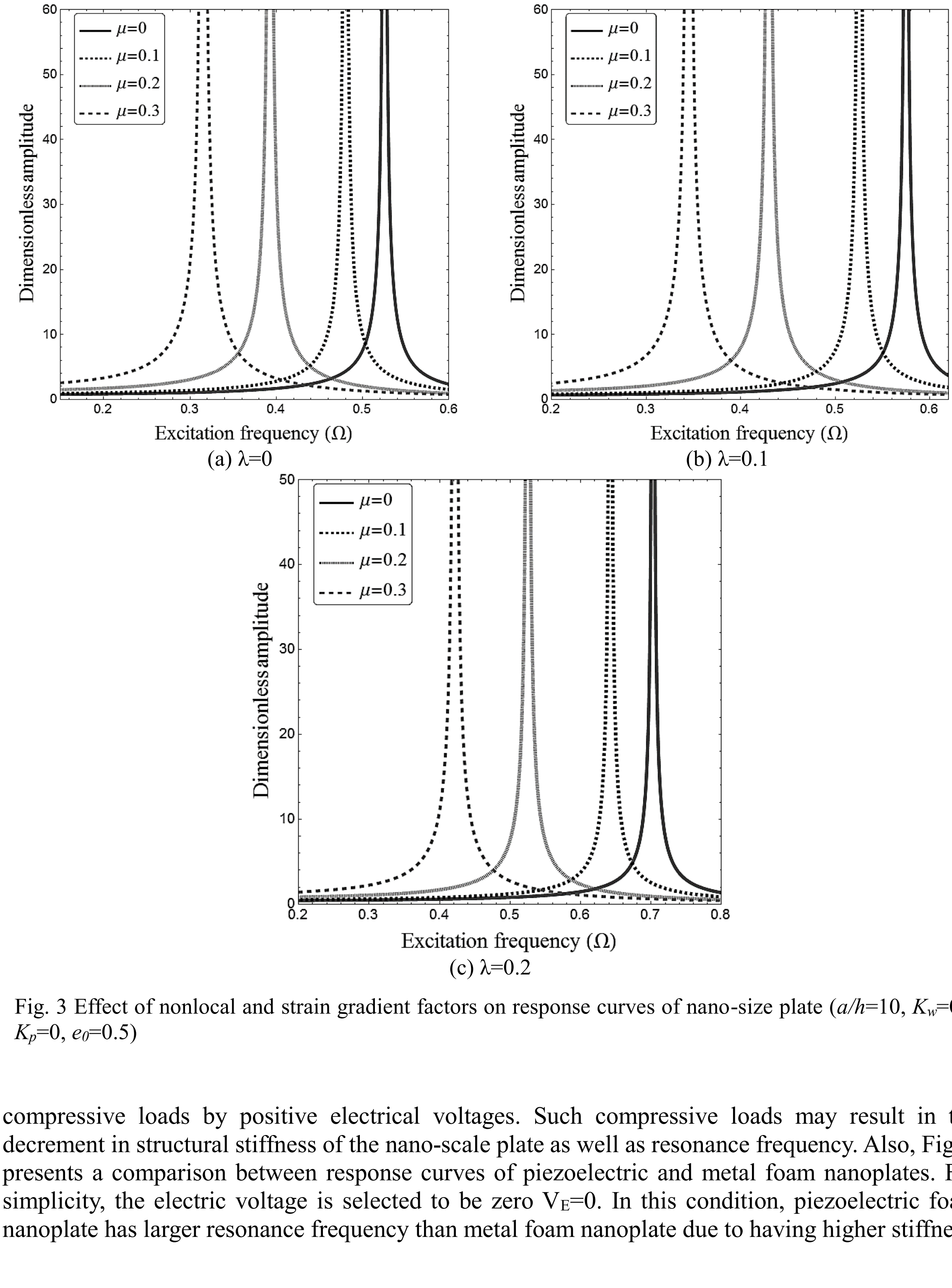

Fig. 3 Effect of nonlocal and strain gradient factors on response curves of nano-size plate (a/h=10, K_w=0, K_p=0, e_0=0.5)

compressive loads by positive electrical voltages. Such compressive loads may result in the decrement in structural stiffness of the nano-scale plate as well as resonance frequency. Also, Fig. 5 presents a comparison between response curves of piezoelectric and metal foam nanoplates. For simplicity, the electric voltage is selected to be zero V_E=0. In this condition, piezoelectric foam nanoplate has larger resonance frequency than metal foam nanoplate due to having higher stiffness.

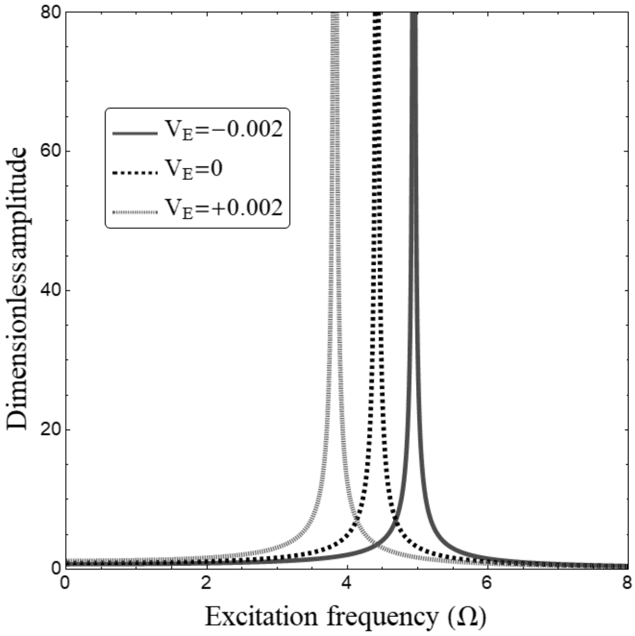

Fig. 4 Effect of applied electric voltage on response curves (*a/h*=20, $\mu=0.2$, $\lambda=0$, e_0=0.2)

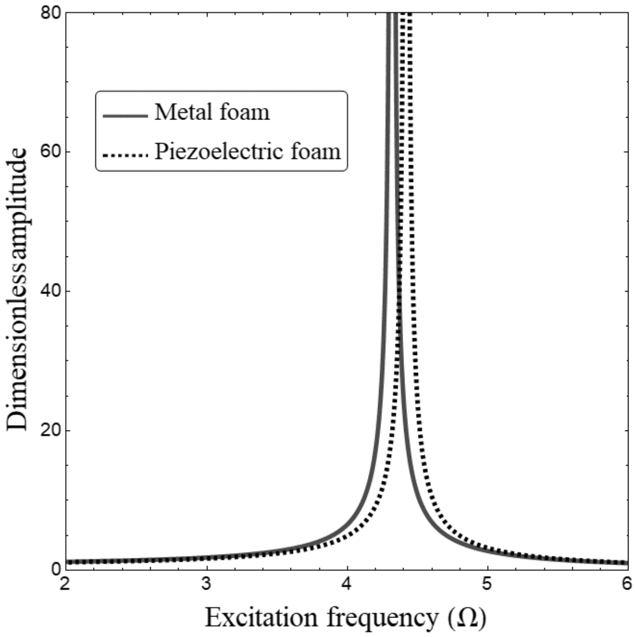

Fig. 5 Comparison between response curves of piezoelectric and metal foam nano-size plates (*a/h*=20, $\mu=0.2$, $\lambda=0$, e_0=0.2, V_E=0)

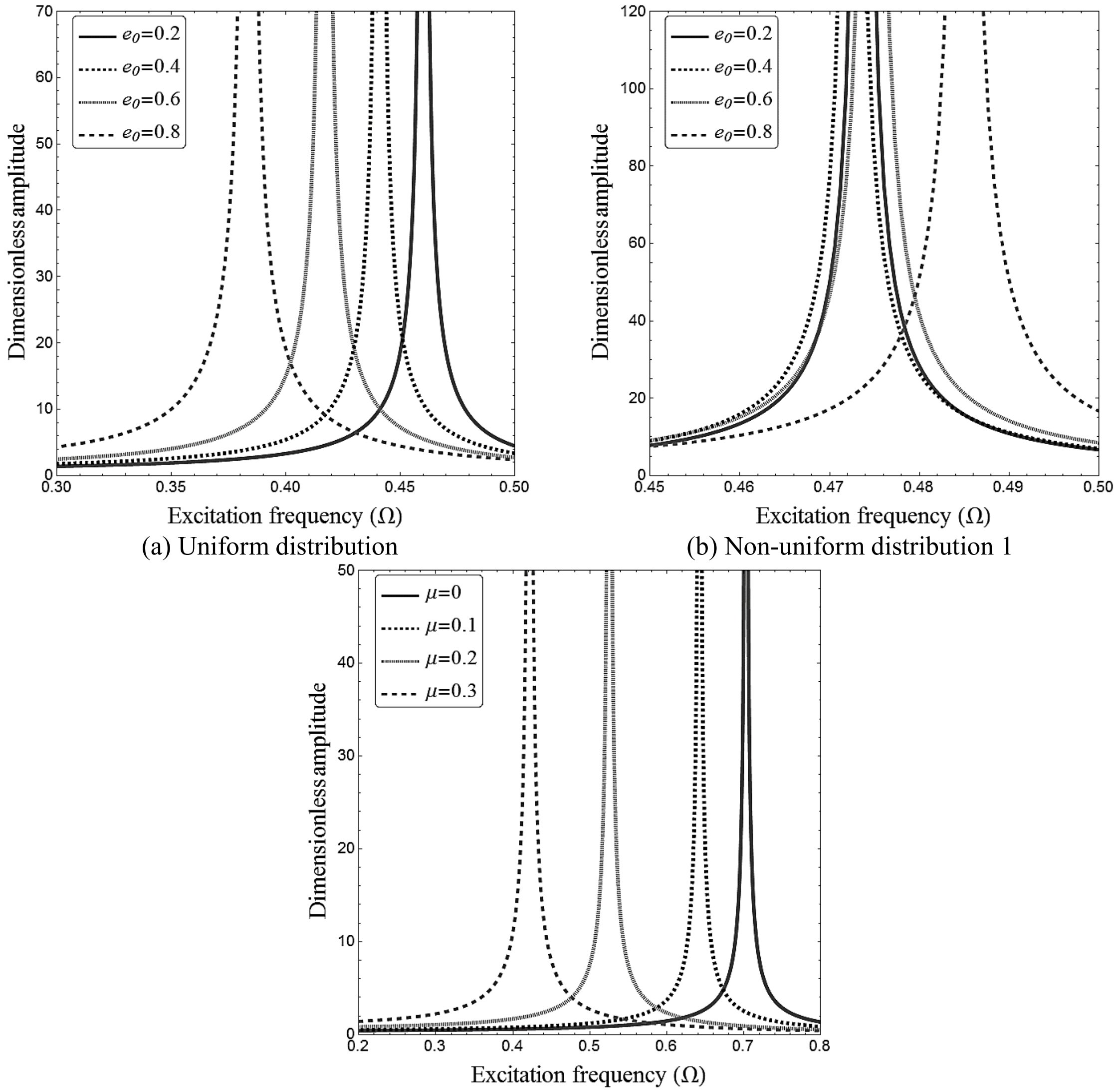

(a) Uniform distribution

(b) Non-uniform distribution 1

(c) Non-uniform distribution 2

Fig. 6 Effect of pore factor and distribution on response curves of the nano-size metal foam plate (a/h=10, K_w=0, K_p=0, $\mu=0.2$, $\lambda=0.1$)

In Fig. 6 one can see the response curves of metal foam plate system with different porosity coefficients and dispersions. Effect of surrounding medium is neglected for this figure. It can be understand from Fig. 6 that resonance frequency of system will reduce or increase with pore coefficient. But, this variation relies on the type of pore dispersion in thickness of nanoplates. Uniform pore type gives higher resonance frequencies than other pore types.

In Fig. 7, normalized deflection variation pursuant to dynamical loading frequency based upon different elastic substrate factors has been explored for simple-supported nano-size plates by

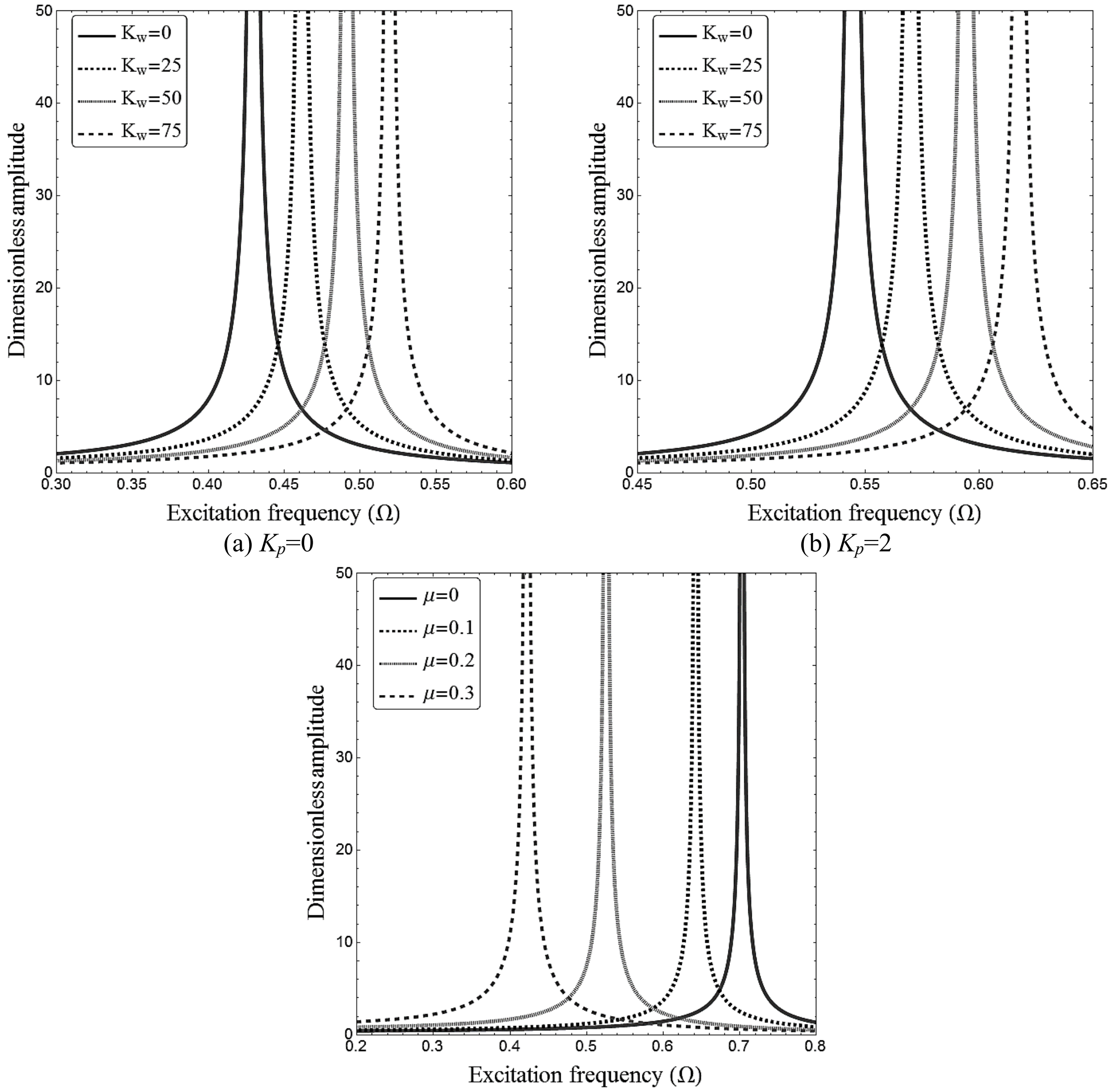

(a) K_p=0

(b) K_p=2

(c) K_p=5

Fig. 7 Response curves of the nano-size plate according to a variety of foundation parameters (a/h=10, $\mu=0.2$, e_0=0.5)

assuming a/h=10, $\mu=0.2$, e_0=0.5. It is found that increasing the substrate factors leads to greater non-dimension resonance frequencies. Indeed, by increasing in substrate factors, the resonance frequency magnitude will be shifted to higher values and dynamical deflections will reduce.

In Fig. 8, the response curves of a nano-size piezoelectric foam plate due to periodic dynamical loading for various temperature rises have been plotted at μ=0.2, e_0=0.2. It is seen from the figure that increasing temperature yields smaller resonance frequency, because of the reduction in stiffness of nano-size plate. Therefore, considering thermal environments is vital for obtaining the best mechanical performances of nanostructures under dynamic loads.

Table 2 Verification study on normalized vibrational frequencies of nano-scale graded plates with various nonlocal factors

a/h	μ				
		a/b=1		a/b=2	
		Natarajan *et al.* (2012)	present	Natarajan *et al.* (2012)	present
10	0	0.0441	0.043823	0.1055	0.104329
	1	0.0403	0.04007	0.0863	0.085493
	2	0.0374	0.037141	0.0748	0.074174
	4	0.0330	0.032806	0.0612	0.060673
20	0	0.0113	0.011256	0.0279	0.027756
	1	0.0103	0.010288	0.0229	0.022722
	2	0.0096	0.009534	0.0198	0.019704
	4	0.0085	0.008418	0.0162	0.016110

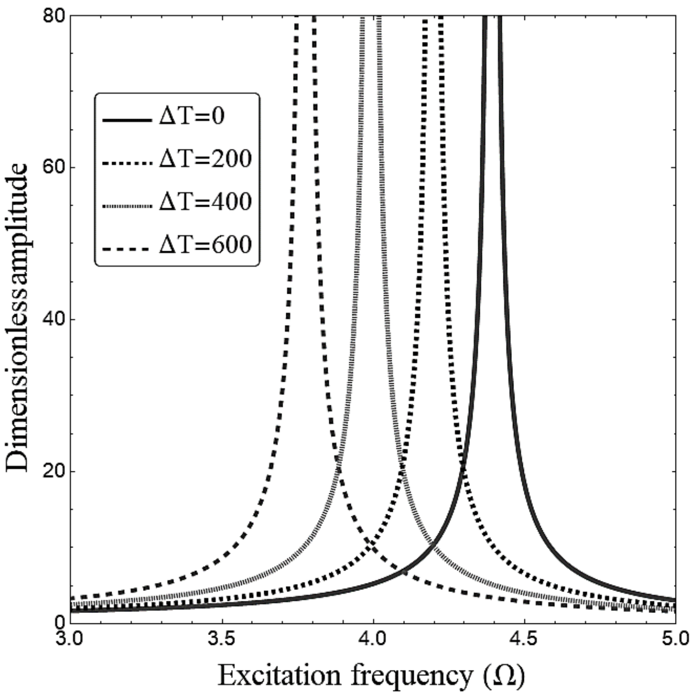

Fig. 8 Response curves of the nano-size plate according to a variety of temperature changes (*a/h*=20, $\mu=0.2$, e_0=0.2)

Acknowledgements

The authors would like to thank Mustansiriyah university (www.uomustansiriyah.edu.iq) Baghdad-Iraq for its support in the present work.

References

Addou, F.Y., Meradjah, M., Bousahla, M.A.A., Benachour, A., Bourada, F., Tounsi, A. and Mahmoud, S.R. (2019), "Influences of porosity on dynamic response of FG plates resting on Winkler/Pasternak/Kerr foundation using quasi 3D HSDT", *Comput. Concrete*, **24**(4), 347-367.

Ahmed, R.A., Fenjan, R.M. and Faleh, N. (2019), "Analyzing post-buckling behavior of continuously graded FG nanobeams with geometrical imperfections", *Geomech. Eng.*, **17**(2), 175-180. https://doi.org/10.12989/gae.2019.17.2.175.

Atmane, H.A., *et al.* (2017), "Effect of thickness stretching and porosity on mechanical response of a functionally graded beams resting on elastic foundations", *Int. J. Mech. Mater. Des.*, **13**(1), 71-84.

Al-Maliki, A.F., Faleh, N.M. and Alasadi, A.A. (2019), "Finite element formulation and vibration of nonlocal refined metal foam beams with symmetric and non-symmetric porosities", *Struct. Monit. Maint.*, **6**(2), 147-159. https:// doi.org/10.12989/smm.2019.6.2.147.

Attia, A., *et al.* (2018), "A refined four variable plate theory for thermoelastic analysis of FGM plates resting on variable elastic foundations", *Struct. Eng. Mech.*, **65**(4), 453-464.

Atmane, H.A., Tounsi, A., Bernard, F .and Mahmoud, S.R. (2015), "A computational shear displacement model for vibrational analysis of functionally graded beams with porosities", *Steel Compos. Struct.*, **19**(2), 369-384. https://doi.org/10.12989/scs.2015.19.2.369.

Chen, D., Yang, J. and Kitipornchai, S. (2015), "Elastic buckling and static bending of shear deformable functionally graded porous beam", *Compos. Struct.*, **133**, 54-61. https://doi.org/10.1016/j.compstruct.2015.07.052.

Chen, D., Kitipornchai, S. and Yang, J. (2016), "Nonlinear free vibration of shear deformable sandwich beam with a functionally graded porous core", *Thin-Wall. Struct.*, **107**, 39-48. https://doi.org/10.1016/j.tws.2016.05.025.

Ebrahimi, F., Dabbagh, A. and Rastgoo, A. (2019), "Vibration analysis of porous metal foam shells rested on an elastic substrate", *J. Strain Anal. Eng. Des.*, **54**(3), 199-208.

El-Hassar, S.M., Benyoucef, S., Heireche, H. and Tounsi, A. (2016), "Thermal stability analysis of solar functionally graded plates on elastic foundation using an efficient hyperbolic shear deformation theory", *Geomech. Eng.*, **10**(3), 357-386. https://doi.org/10.12989/gae.2016.10.3.357.

Eltaher, M.A., Khater, M.E., Park, S., Abdel-Rahman, E. and Yavuz, M. (2016), "On the static stability of nonlocal nanobeams using higher-order beam theories", *Adv. Nano Res.*, **4**(1), 51-64. http://dx.doi.org/10.12989/anr.2016.4.1.000.

Elmerabet, A.H., Heireche, H., Tounsi, A. and Semmah, A. (2017), "Buckling temperature of a single-walled boron nitride nanotubes using a novel nonlocal beam model", *Adv. Nano Res.*, **5**(1), 1-12. https://doi.org/10.12989/anr.2017.5.1.001.

Eringen, A.C. (1983), "On differential equations of nonlocal elasticity and solutions of screw dislocation and surface waves", *J. Appl. Phys.*, ***54***(9), 4703-4710. https://doi.org/10.1063/1.332803.

Fenjan, R.M., Ahmed, R.A., Alasadi, A.A. and Faleh, N.M. (2019), "Nonlocal strain gradient thermal vibration analysis of double-coupled metal foam plate system with uniform and non-uniform porosities", *Coupled Syst. Mech.*, **8**(3), 247-257. https://doi.org/10.12989/csm.2019.8.3.247.

Li, C., Guo, L., Shen, J.P., He, Y.P. and Ju, H. (2013), "Forced vibration analysis on nanoscale beams accounting for effective nonlocal size effects", *Adv. Vibr. Eng.*, **12**(6), 623-633.

Li, L. and Hu, Y. (2016), "Wave propagation in fluid-conveying viscoelastic carbon nanotubes based on nonlocal strain gradient theory", *Comput. Mater. Sci.*, **112**, 282-288.

https://doi.org/10.1016/j.commatsci.2015.10.044.

Liu, J., Chen, L., Xie, F., Fan, X. and Li, C. (2016), “On bending, buckling and vibration of graphene nanosheets based on the nonlocal theory”, *Smart Struct. Syst.*, **17**(2), 257-274.

Li, C., Lai, S.K. and Yang, X. (2019), “On the nano-structural dependence of nonlocal dynamics and its relationship to the upper limit of nonlocal scale parameter”, *Appl. Math. Model.*, **69**, 127-141.

Lim, C.W., Zhang, G. and Reddy, J.N. (2015), “A higher-order nonlocal elasticity and strain gradient theory and its applications in wave propagation”, *J. Mech. Phys. Solids*, **78**, 298-313. https://doi.org/10.1016/j.jmps.2015.02.001.

Mahmoudi, A., *et al.* (2019), “A refined quasi-3D shear deformation theory for thermo-mechanical behavior of functionally graded sandwich plates on elastic foundations”, *J. Sandw. Struct. Mater.*, **21**(6), 1906-1929.

Mechab, I., Mechab, B., Benaissa, S., Serier, B. and Bouiadjra, B.B. (2016), “Free vibration analysis of FGM nanoplate with porosities resting on Winkler Pasternak elastic foundations based on two-variable refined plate theories”, *J. Braz. Soc. Mech. Sci. Eng.*, **38**(8), 2193-2211. https://doi.org/10.1007/s40430-015-0482-6.

Medani, M., *et al.* (2019), “Static and dynamic behavior of (FG-CNT) reinforced porous sandwich plate”, *Steel Compos. Struct*., **32**(5), 595-610.

Meksi, R., *et al*. (2019), “An analytical solution for bending, buckling and vibration responses of FGM sandwich plates”, *J. Sandw. Struct. Mater*., **21**(2), 727-757.

Merazi, M., Hadji, L., Daouadji, T.H., Tounsi, A. and Adda Bedia, E.A. (2015), “A new hyperbolic shear deformation plate theory for static analysis of FGM plate based on neutral surface position”, *Geomech. Eng,*, **8**(3), 305-321. https://doi.org/10.12989/gae.2015.8.3.305.

Natarajan, S., Chakraborty, S., Thangavel, M., Bordas, S. and Rabczuk, T. (2012), “Size-dependent free flexural vibration behavior of functionally graded nanoplates”, *Comput. Mater. Sci.*, **65**, 74-80. https://doi.org/10.1016/j.commatsci.2012.06.031.

Sadoun, M., Houari, M.S.A., Bakora, A., Tounsi, A., Mahmoud, S.R. and Alwabli, A.S. (2018), “Vibration analysis of thick orthotropic plates using quasi 3D sinusoidal shear deformation theory”, *Geomech. Eng.*, **16**(2), 141-150. https://doi.org/10.12989/gae.2018.16.2.141.

Sayyad, A.S. and Ghugal, Y.M. (2018), “An inverse hyperbolic theory for FG beams resting on Winkler-Pasternak elastic foundation”, *Adv. Aircraft Spacecraft Sci.*, **5**(6), 671-689. https://doi.org/10.12989/aas.2018.5.6.671.

Semmah, A., *et al*. (2019), “Thermal buckling analysis of SWBNNT on Winkler foundation by non local FSDT”, *Adv. Nano Res*., **7**(2), 89-98.

Shokravi, M. (2017), “Buckling analysis of embedded laminated plates with agglomerated CNT-reinforced composite layers using FSDT and DQM”, *Geomech. Eng.*, **12**(2), 327-346. https://doi.org/10.12989/gae.2017.12.2.327.

Sobhy, M. and Radwan, A.F. (2017), “A new quasi 3D nonlocal plate theory for vibration and buckling of FGM nanoplates”, *Int. J. Appl. Mech.*, **9**(01), 1750008. https://doi/abs/10.1142/S1758825117500089.

Wattanasakulpong, N. and Ungbhakorn, V. (2014), “Linear and nonlinear vibration analysis of elastically restrained ends FGM beams with porosities”, *Aerosp. Sci. Technol.*, **32**(1), 111-120. https://doi.org/10.1016/j.ast.2013.12.002.

Xiao, W., Li, L. and Wang, M. (2017), “Propagation of in-plane wave in viscoelastic monolayer graphene via nonlocal strain gradient theory”, *Appl. Phys. A*, **123**(6), 388. https://doi.org/10.1007/s00339-017-1007-1.

Yazid, M., *et al*. (2018), “A novel nonlocal refined plate theory for stability response of orthotropic single-layer graphene sheet resting on elastic medium”, *Smart Struct. Syst*., **21**(1), 15-25.

Younsi, A., Tounsi, A., Zaoui, F.Z., Bousahla, A.A. and Mahmoud, S.R. (2018), “Novel quasi-3D and 2D shear deformation theories for bending and free vibration analysis of FGM plates”, *Geomech. Eng.*, **14**(6), 519-532. https://doi.org/10.12989/gae.2018.14.6.519.

Zenkour, A.M. and Abouelregal, A.E. (2015), “Thermoelastic interaction in functionally graded nanobeams subjected to time-dependent heat flux”, *Steel Compos. Struct.*, **18**(4), 909-924. https://doi.org/10.12989/scs.2015.18.4.909.

Zhu, X. and Li, L. (2017), “Closed form solution for a nonlocal strain gradient rod in tension”, *Int. J. Eng.*

Sci., **119**, 16-28. https://doi.org/10.1016/j.ijengsci.2017.06.019.

TY